31st Annual International Conference of the IEEE EMBS
Minneapolis, Minnesota, USA, September 2-6, 2009

Feasibility of Regional and Global Left Ventricular Shape Analysis From Real-Time 3d Echocardiography

Francesco Maffessanti, Lissa Sugeng, Masaaki Takeuchi, Lynn Weinert, Victor Mor-Avi, Roberto M. Lang, Enrico G. Caiani

Abstract— **Combined assessment of left ventricular (LV) shape and function could provide new insights into the process of LV remodeling. Real-time 3D echocardiography (RT3DE) allows rapid and accurate semi-automated extraction of LV endocardial surfaces. Our aims were to quantify LV morphology both globally and regionally, using new ellipsoidal (E), spherical (S) and conical (C) shape indices, in a large population in order to define normal values.**

During systole the LV became less spherical and more conical, while E index remained unchanged. LV volume estimation was more affected by operator subjectivity than C and S indexes computation.

These results constitute a reference for future comparisons with serial follow-up of patients during LV remodeling.

I. Introduction

The relationship between left ventricular (LV) function and shape is well described in the literature and it is based on the pathophysiological process of remodeling. This process has been observed in several pathological conditions [1, 2, 3, 4]. Despite the potential ability of LV shape analysis to provide both additional information complementary to LV function and new insights into the process of LV remodeling, LV shape is not quantified in clinical practice. .

In the past, quantitative approaches to shape analysis have been applied to different imaging techniques [4, 5, 6, 7, 8, 9, 10]. Unfortunately, previously proposed indices relied on tedious and subjective manual tracing and had intrinsic limitations in describing the 3D shape from 2D images using a priori geometric assumptions.

Real-time 3D echocardiography (RT3DE) could overcome some of these limitations, as it allows rapid acquisition of 3D datasets and provides the basis for an accurate estimation of LV size, function and mass [11]. However, while currently available commercial software allows reliable LV functional analysis, no tools are available for LV shape quantification.

Accordingly, the aims of this study were: 1) to develop a technique for the quantification of a new class of 3D global and regional LV shape indices from RT3DE datasets; 2) to test the performance of this technique on computer-simulated 3D shapes; 3) to study the LV shape changes occurring in the human heart throughout the cardiac cycle.

Manuscript received April 23, 2009.

F. M and E. G. C. are with the Politecnico di Milano, Dipartimento di Bioingegneria, Milano, Italy

L. S., V. M. and R. M. L. are with the Department of Medicine, University of Chicago, Chicago, Illinois, U.S.A.

M. T. is with the University of Occupational and Environmental Health, Kitakyushu, Japan.

II. Methods

A. Imaging Protocol

A group of 147 normal subjects (age 38±19, range: 3÷88 years; 93M; ejection fraction=55±5%; normalized LV volumes: end-diastolic (ED)=67±15ml/m^2, end-systolic (ES)=30±8ml/m^2) was enrolled at the University of Chicago Medical Center, Chicago, IL. The protocol was approved by the Institutional Review Board and informed consent was obtained from all study subjects.

Transthoracic RT3DE imaging was performed using a iE33 system equipped with an X3 probe (Philips Medical). LV endocardial surfaces were semi automatically extracted using commercial software (4D LV Analysis, TomTec Imaging Systems) and, for each frame, the detected surface was used to calculate the 3D shape indices described below.

B. 1D LV surface description

LV shape indices were obtained using custom analysis software, implemented in the Matlab environment (MathWorks Inc, Natick, MA). First, the 3D LV endocardial surface was represented as a 1D signal by helical sampling using a modified formulation of the procedure previously described in detail elsewhere [6].

Figure 1 depicts the steps required to perform this analysis: a) for each frame, the principal inertial axes of the extracted LV cavity were computed. A cylindrical floating reference system was defined for each frame, with its unit vector **v** aligned with the LV long axis (LAX); b) the endocardial surface was sampled along a helical path aligned with **v** from apex to base, using 64 windings and 36 samples per winding: the resultant 1D signal $s(\theta)$ describes the Euclidean distance from LAX to the endocardial surface, normalized by LAX length; c) to obtain the signal $s(\theta)$ with a constant number of samples, independent of LV dimensions, the angular coordinate η, ranging from 0 (apex) to 1 (base), was considered, normalizing θ by its maximum value ($\theta_{max}=64 \bullet 2\pi$).

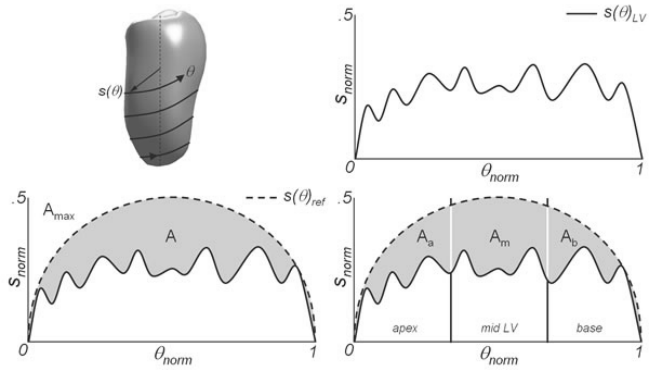

Fig. 1. The LV endocardial surfaces and the sampling helix: $s(\theta)$ represents the distance between LV long axis (LAX) and endocardial surface (top left); the signal $s(\theta)_{LV}$ is obtained by normalizing $s(\theta)$ by LAX, while η normalizing the angular coordinate θ (top right); the area A between $s(\theta)$ and a reference signal $s(\theta)_{REF}$ measures the degree of dissimilarity between the two signals at global (bottom left) and apical, medial and basal levels (bottom right).

The resultant signal $s(\eta)$ and its reference system are dependent on LV shape and aspect ratio, but independent of LV size.

C. Reference shape definition

A new class of global 3D shape indices was defined by measuring the degree of similarity between $s(\eta)$, computed from the LV ($s(\eta)_{LV}$), and obtained from a reference 3D shape using the same helical sampling procedure ($s(\eta)_{ref}$). In order to compute $s(\eta)_{ref}$, three different shapes were considered: a sphere, an ellipsoid and a cone with elliptical section. These shapes were created while preserving the same principal moments of inertia of the LV being analyzed, under the hypothesis that LV aspect ratio is strictly related to LV cavity spatial distribution. To this effect, the reference signal relevant to the sphere, independent of LV aspect ratio (ie, aspect ratio of 1), was defined as a semi-circular signal:

$$\rho(\eta)_S = \sqrt{.5^2 - (\eta - .5)^2} \tag{1}$$

The reference signals relevant to the ellipsoid and the cone were obtained by modulating the signal shape(η), associated with a reference shape with aspect ratio of 1, with the signal aspect(η), related to LV aspect ratio:

$$s(\eta)_{ref} = aspect(\eta) \cdot shape_{ref}(\eta) \tag{2}$$

In particular, the signal *aspect(η)* was defined as:

$$aspect(\eta) = \frac{B}{H} \cdot \sqrt{\frac{1-e}{1-e \cdot sin^2(128\pi \cdot \eta)}} \tag{3}$$

where e is the short axis eccentricity computed as:

$$e = 1 - \frac{A^2}{B^2} \tag{4}$$

A and B are the minor and major axis lengths of the elliptical section of the reference shape, and H represents the length of the third axis for the ellipsoid or the height for the cone.

After computing the moments of inertia of the LV (ie, I_x, I_y and I_z), the values of A, B, and H were obtained as:

$$A = \sqrt{\alpha \cdot \frac{-I_x + I_y + I_z}{LVV}} \quad B = \sqrt{\beta \cdot \frac{+I_x - I_y + I_z}{LVV}} \quad H = \sqrt{\chi \cdot \frac{+I_x + I_y - I_z}{LVV}} \tag{5}$$

with $\alpha=\beta=\chi=5/2$ for the ellipsoid, $\alpha=\beta=10/3$ and $\chi=40/3$ for the cone and LVV representing the LV volume.

D. Shape indices computation

Global spherical (S), ellipsoidal (E), and conical (C) 3D shape indices in dimensionless units were computed as:

$$Global\ shape\ index = 1 - \frac{A}{A_{max}} \tag{6}$$

where A is the area between the corresponding $s(\eta)_{REF}$ and $s(\eta)_{LV}$, while A_{max} is the total area in the (s,η) plane, equal to 0.5 by definition (Figure 1, bottom left).

Using the same formulation, three regional 3D shape indices where also computed by subdividing the (s,η) plane into three portions of equal size (Figure 1, bottom right):

$$Regional\ shape\ index = 1 - 3\frac{A_i}{A_{max}} \tag{7}$$

where A_i is the area between the corresponding $s(\eta)_{REF}$ and $s(\eta)_{LV}$ in the apical (A_a), medial (A_m) and basal (A_b) regions.

E. Computer simulation

In order to test the performance of this technique, a series of computer-simulated 3D objects was generated (Figure 2). The geometrical characteristics of the considered objects are reported in figure 2. In particular, we considered: 1) two spheres, E1 and E2, with different radius; 2) an ellipsoid, E3, with same circular section of E2 but elliptical in the long axis direction; 3) an ellipsoid, E4, with two elliptical cross-sections; 4) two circular cones, C1 and C2, with the same height but different radius; 5) a cone, C3, having the same height of C2 but elliptical section; 6) a frustum, C4, with the same major basis and height of C3.

	E1	E2	E3	E4	C1	C2	C3	C4
L_2/L_1	1	1	.8	.8	.25	.33	.33	.33
L_3/L_1	1	1	.8	.6	.25	.33	.17	.17
L_3/L_1	1	1	1	.75	1	1	.5	.5
V_n^2	3.4	1	1.2	.9	.4	.75	.4	1

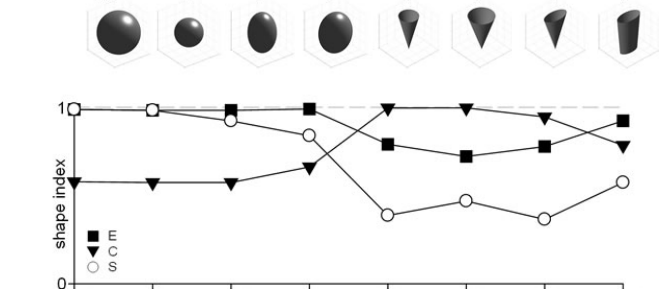

Fig. 2. Spherical (S), conical (C) and ellipsoidal (E) shape indices values calculated for simulated objects, with the corresponding geometrical characteristics: L_1, L_2 and L_3 represent the principal axis dimensions ($L_1>L_2>L_3$) and V_n the volume of each object normalized to the volume of E_2.

To test for volume independence of the computed shape indices, the objects E1 and E2, and C1 and C2 were compared. To verify the ability of the technique in recognizing the 3D shape category (i.e. an ellipsoid or a cone) the objects E1-E4 and C1-C4 were used, for the E and S indices, and for the C index, respectively.

F. Statistical analysis

Wilcoxon signed-ranks test ($p<.01$) was applied to test for global and regional shape changes through the cardiac cycle, considering the ED and the ES values of each index.

In addition, for a subgroup of 50 subjects, analysis was performed by two different operators. The inter-observer variability, both for volume and shape indices, was assessed as coefficient of variation (CV%):

$$CV(\%) = \frac{1}{N}\sum_{i=1}^{N}\frac{\sigma(x_A, x_B)}{\bar{x}} \cdot 100\% \quad (8)$$

where $\sigma(x_A, x_B)$ is the standard deviation and $\bar{x}$ the mean.

III. RESULTS

A. Simulated objects

The index E (Figure 2, black squares), equal to 1 for all the ellipsoidal objects, correctly recognized the object category, independently of volume and sections. The index S (white circles) was equal to 1 for the two spheres E1 and E2, independently of their volume. When one section was elliptical (E3), sphericity started decreasing to S=.92; when both sections were not circular (E4), S strongly decreased to S=.83. The shape index C (black triangle) was able to recognize the 3 cones C1-C3, independently of their volume and transversal aspect ratio. The combined use of different shape indices allowed the description of the conical frustum as a mixture of an ellipsoid (E=.92) and a cone (C=.78).

B. Global shape analysis

Shape computation was feasible in all study subjects. The analysis was completely automated once the surfaces were extracted, and required less than one minute for one complete cardiac cycle on a standard laptop.

Figure 3 shows an example of the S, E and C shape indices computed throughout one cardiac cycle.

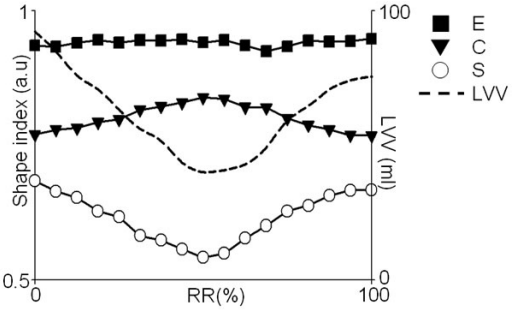

Fig 3. Changes in the 3D shape indices (ellipsoidal E, spherical S and conical C) throughout one cardiac cycle, together with the corresponding LV volume (LVV – dashed line, secondary y-axis), in a representative subject.

Index E remained approximately constant, suggesting its independence of LV volume. Conversely, indices S and C varied throughout the cardiac cycle in opposing phases. In addition, S and C reached their minimum or maximum values simultaneously at the end of ejection. The mean ED and ES values calculated for each shape index are presented in figure 4.

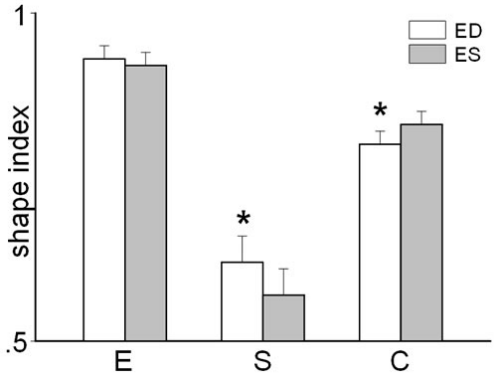

Fig. 4. Mean values of ellipsoidal (E), spherical (S) and conical (C) shape indices calculated at ED and at ES (Wilcoxon signed-ranks test * : $p<.01$ ED vs ES).

The LV was found less spherical and more conical during systole, while a more spherical morphology was restored during diastole. Interestingly, independently of cardiac phase, the LV shape is best described by an ellipsoid.

C. Regional shape analysis

Table 1 shows averaged regional shape indices E, S and C, computed at ED and ES.

TABLE I

		E	S	C
Apex	ED	.94±.03	.62±.03	.76±.04*
	ES	.92±.03	.56±.04*	.81±.04
Mid	ED	.95±.02	.51±.05	.76±.03
	ES	.94±.02	.45±.05*	.81±.04*
Base	ED	.88±.02	.74±.05	.88±.01
	ES	.89±.02	.69±.06*	.88±.01*

Regional shape indices at ED and at ES. Values expressed as mean ± SD (Wilcoxon signed-ranks test * : $p<.01$ ED vs ES).

Similarly to the global results, index E showed no significant differences between ED and ES, while. regional changes in the indices S and C were noticed. ED values of S were higher than the ES values in all regions; apical and medial values of the C index were found lower at ES than at ED, while values at base remained constant.

D. Inter-observer variability

The coefficients of variation relevant to LV volumes, conicity and sphericity indexes are shown in Figure 5.

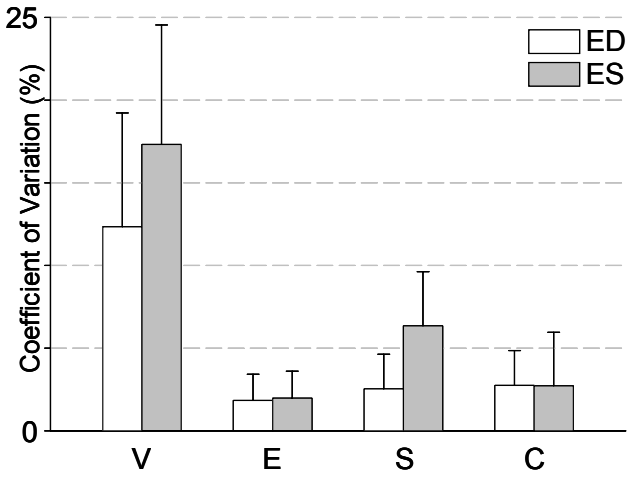

Fig. 5. The coefficient of variation relevant to ED and ES values for LV volume (V), ellipsoidal (E), spherical (S) and conical (C) shape indices.

Our results showed that LV volume estimation is more affected by operator subjectivity than shape indices. In particular E value seemed the least affected (ED: CV_E=1.2%; ES: CV_E=1.3%).

IV. Conclusions

We evaluated both global and regional LV shape in a relatively large group of normal subjects using a new technique based on analysis of transthoracic RT3DE images. The global 3D LV shape information was used by reducing problem complexity to a single dimension but considering the shape ratio.

Despite the high inter-operator variability in LV endocardial tracing, influencing LV volume computation, the computed indices were found to be only minimally affected by this factor.

Interestingly, the relationship with changes in LV volume throughout the cardiac cycle was different for each LV shape index: while ellipsoidal index remained approximately constant, suggesting its independence of LV volume, during systole, sphericity decreased and conicity increased. Regional analysis revealed that in normal subjects, shape indices behaved similarly at all LV levels.

In summary, 3D LV shape analysis of RT3DE images may provide useful information on LV morphology and help to better understand its relation with LV function, in particular to indentify abnormalities in LV function. The results of this study constitute a reference for future comparisons in serial follow up studies of patients during LV remodeling or patients with congenital heart disease.

References

[1] Ross J Jr, McCullagh WH, "Nature of enhanced performance of the dilated left ventricle in the dog during chronic volume overloading," *Circ Res*, vol. 30, no. 5, pp. 549-56, May 1972.

[2] Ricci DR, "Afterload mismatch and preload reserve in chronic aortic regurgitation," *Circulation*, vol. 66, no. 4, pp. 826-34, Oct. 1982.

[3] Pfeffer MA, Braunwald E, "Ventricular remodeling after myocardial infarction," *Circulation*, vol. 81, no. 4, pp. 1161-72, Apr. 1990.

[4] Harjai KJ, Edupuganti R, Nunez E, Turgut T, Scott L, Pandian NG, "Does left ventricular shape influence clinical outcome in heart failure?," *Clin Cardiol*, vol. 23, no. 11, pp. 813–9, Nov. 2000.

[5] Gibson DG, Brown DJ, "Continuous assessment of left ventricular shape in man," *Br Heart J*, vol. 37, no. 9, pp. 904-10, Sep. 1975.

[6] Azhari H, Sideman S, Beyar R, Grenadier E, Dinnar U, "An analytical descriptor of three-dimensional geometry: application to the analysis of the left ventricle shape and contraction," *IEEE Trans Biomed Eng*, vol. 34, no. 5, pp. 345-55, May 1987.

[7] Mancini GB, DeBoe SF, Anselmo E, Simon SB, LeFree MT, Vogel RA. "Quantitative regional curvature analysis: an application of shape determination for the assessment of segmental left ventricular function in man," *Am Heart J*, vol. 113, pp. 326-34, Feb 1987.

[8] Kass DA, Traill TA, Keating M, Altieri PI, Maughan WL, "Abnormalities of dynamic ventricular shape change in patients with aortic and mitral valvular regurgitation: assessment by Fourier shape analysis and global geometric indices," *Circ Res*, vol. 62, pp. 127-38, 1988.

[9] Chan SY, Mancini GB, Fu Y, O'Brien DW, Armstrong PW, "Novel methodology for echocardiographic quantification of cardiac shape," *Can J Cardiol*, vol. 13, no. 2, pp. 153-9, Feb. 1997.

[10] Mannaerts HF, van der Heide JA, Kamp O, Stoel MG, Twisk J, Visser CA, "Early identification of left ventricular remodeling after myocardial infarction, assessed by transthoracic 3D echocardiography," *Eur Heart J*, vol. 25, no. 8, pp. 680-7, Feb. 2004.

[11] Lang RM, MorAvi V, Sugeng L, Nieman PS, Sahn DJ. "Three dimensional echocardiography. The benefits of the additional dimension," *J Am Coll Cardiol*, vol. 48, no. 10, pp. 2053-69, Nov. 2006.